

Integrating fixed and mobile arterial roadway data sources for transportation analysis

Alexander Bigazzi abigazzi@pdx.edu

Wei Feng; wfeng@pdx.edu

Adam Moore; adam.moore@pdx.edu

Miguel Figliozzi; figliozzi@pdx.edu

Department of Civil and Environmental Engineering

Portland State University

P.O. Box 751-CEE, Portland, OR, 97207

Ph: 503-725-4282

PRESENTED at the Workshop on Big Data and Urban Informatics

National Science Foundation, August 11-12, 2014. University of Illinois at Chicago, Chicago, IL

<http://urbanbigdata.uic.edu/proceedings/>

ABSTRACT

Fixed-site and mobile data sources have distinct strengths for representing roadway conditions, and unique insights can be generated by combining the two. Ongoing research on an urban arterial roadway corridor combines distinct data sources for multi-criteria transportation facility performance assessment. The roadway is instrumented with an adaptive traffic signal system collecting signal phase and vehicle count data and mid-block radar detectors recording high-resolution vehicle counts, speeds, and classifications. Transit buses on the corridor record stop-level vehicle position and passenger activity data, and air quality has been measured with deployable roadside monitoring stations and a portable multi-sensor device for travelers. Combinations of these data sources provide new insights about performance of the transit signal priority (TSP) system, relationships between signal operations and roadside air quality, and variations in on-road exposure concentrations.

Keywords: roadway data, performance measures, transit operations, traffic signals, air pollution

1 INTRODUCTION

The most recent U.S. surface transportation act, MAP-21, continues the trend of increasing use of performance measures for analysis of transportation systems. The increasing demands of performance measures along with technological developments have led to an abundance of new data sources available to transportation analysts. Traditional transportation data come from fixed infrastructure elements such as video cameras or embedded inductive loop detectors. Mobile data sources emerged with the gathering of sensor data from fleet vehicles such as transit buses and taxis. The recent proliferation of personal mobile devices expands the opportunities for mobile data collection.

Although there is a profusion of data originating from transportation systems, challenges remain in converting those data into information (Tufté, Bertini, Chee, Fernandez-Moctezuma, & Periasamy, 2010). One underused analytical approach is the integration of fixed and mobile data sources, which each provide a unique view of roadway conditions. Although new analysis

techniques might be required, combining fixed and mobile data can provide a fuller and potentially more accurate representation of conditions (Feng, Bigazzi, Kothuri, & Bertini, 2010).

This paper presents findings based on integrated fixed and mobile data sources on an urban arterial roadway. The use of combined data for multi-criteria transportation facility performance assessment is demonstrated and challenges are discussed. Three separate analyses are presented for 1) performance of a transit signal priority system, 2) relationships between signal operations and roadside air quality, and 3) variations in on-road exposure concentrations. The next section describes the data sources on the corridor, and the following section presents performance measurement results.

2 ROADWAY DATA SOURCES

2.1 Description of the study corridor

This research utilizes existing data streams from an instrumented corridor as well as temporary deployments of stationary and mobile traffic, atmospheric, and air quality monitoring systems. The instrumented corridor is SE Powell Boulevard, an urban arterial in Portland, Oregon. Powell Boulevard (also U.S. Highway 26) connects the Portland downtown and the City of Gresham, a suburban city. Powell Boulevard has two lanes of traffic in each direction for most of its length, and a center turn lane or median for left turns in some sections. Sidewalks are present on both sides of the roadway and there are no bicycle lanes. The street route runs east-west and includes the Ross Island Bridge which crosses over the Willamette River (annual average daily traffic at the bridge is over 60,000 vehicles). The study area is highlighted in Figure 1.

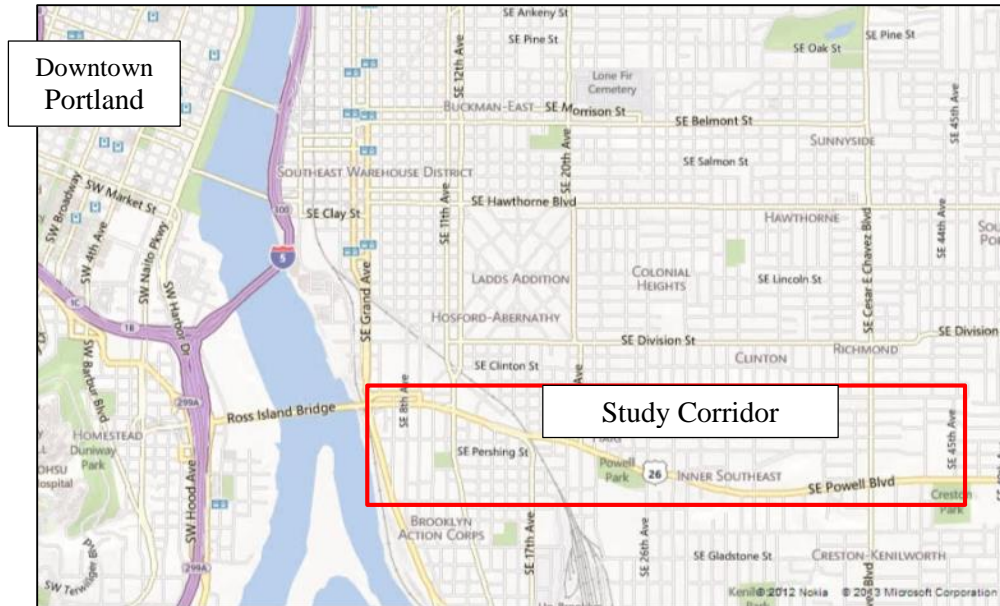


Figure 1. Powell Boulevard study corridor in relation to downtown Portland (bing.com/maps)

Powell Boulevard is regularly congested during peak traffic hours. The morning peak period is in the westbound direction, towards downtown Portland, while the afternoon peak period occurs in the eastbound direction. Powell Boulevard is a key regional commuter facility. This facility is classified as a designated Oregon Department of Transportation (DOT) Region 1 Critical Urban Arterial Corridor. The Ross Island Bridge carries the most traffic volume of any 4-lane facility in the Portland metropolitan area (Figure 2 shows eastbound traffic entering the SE Powell Boulevard corridor from this bridge). Most traffic signals are separated by five or six blocks and in many occasions traffic queues occupy the extension between traffic signals.



Figure 2. Powell Boulevard, traffic moving eastward from the bridge during congested evening hours.

Several bus routes run along Powell Boulevard and are affected by congestion, especially the high frequency bus route 9. Route 9 is within the top five TriMet¹ routes in terms of productivity and passenger demand. The peak periods for Route 9 coincide with general vehicle traffic peaks and occur in the morning for the westbound direction and in the afternoon for the eastbound direction.

Along Powell Boulevard there is a variety of land uses coupled with intense commercial, educational, recreational, and residential activities. For example, Powell City Park is located between SE 22nd and SE 26th Streets; Cleveland High School (1,500 students) is located between SE 26th and SE 27th Streets and its recreational and sports facilities are located between SE 31st and 33rd Streets. In addition, numerous strip malls, popular restaurants, a brewery, a supermarket, and residential apartment complexes are located along Powell Boulevard. Improving the performance of this arterial is difficult due to the competing needs of different types of users such as pedestrians, transit, and private automobiles as well as balancing mobility and accessibility for a diverse array of activities and land uses along the corridor.

¹ TriMet stands for Tri-county Metropolitan area and is the public transit agency serving the three counties that comprise the Portland metropolitan region with a current population estimated around 2,300,000

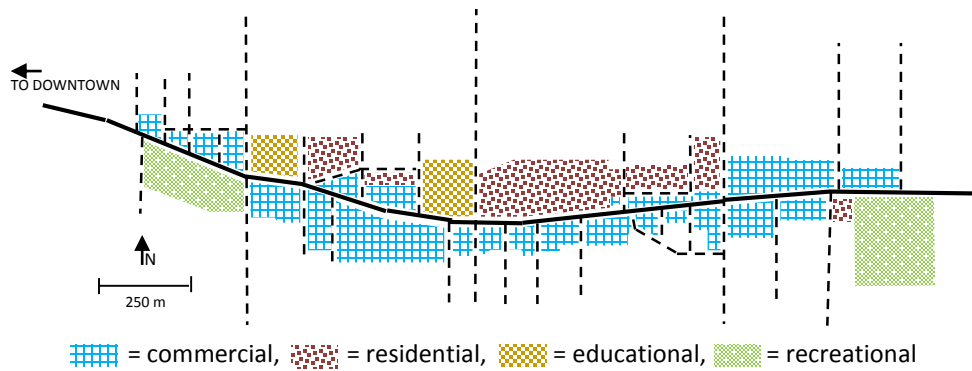


Figure 3. Development zoning along study corridor.

2.2 Fixed traffic data sources

The study corridor was chosen because of a unique set of complementary traffic data technologies. The City of Portland and the Oregon Department of Transportation deployed a state-of-the-art adaptive traffic signal system called SCATS (Sydney Coordinated Adaptive Traffic System-SCATS) between September 2011 and March 2012. SCATS optimizes traffic signals and traffic performance adapting or responding to changes in traffic volumes or conditions along the corridor. The green and red signal durations change throughout the day as SCATS coordinates traffic signals along the entire corridor, enabling the formation of “platoons” of vehicles that move together. Intersection cycle lengths, phase splits, and offsets are optimized on a cycle-by-cycle basis, allowing the entire corridor to adapt to changing traffic trends faster than traditional traffic signal systems. SCATS detectors record vehicle count data for every lane approaching an intersection, as well as all phase timing data.

Digital Wave Radar (DWR) sensors measure arterial traffic volumes, speed, vehicle length, vehicle type, and lane occupancy rate. Two Wavetronix-brand permanent DWR sensors are situated at mid-block locations (between major intersections) along the corridor – one at SE 24th Avenue and one at SE 35th Avenue. DWR sensors quantify vehicle volumes and vehicle types based on length (passenger car versus truck) at the lane level and per direction of travel.

2.3 Transit operations data

The study area includes 22 bus stops in each direction. Route 9 is the primary bus line along the corridor, with additional service from Route 66 and four other routes on cross streets (see Figure 4). Recorded bus stop event data include bus arrival and departure times, passenger activities (boarding and alighting), and vehicle and driver information at each bus stop along the

corridor. Each bus GPS record has a unique ID that can be matched to the bus vehicle data (brand, size, age, mileage, maintenance record, type of UFP filter, actual fuel efficiency, etc.). The bus fleet uses B5 biodiesel (5% biodiesel, 95% petrol diesel).

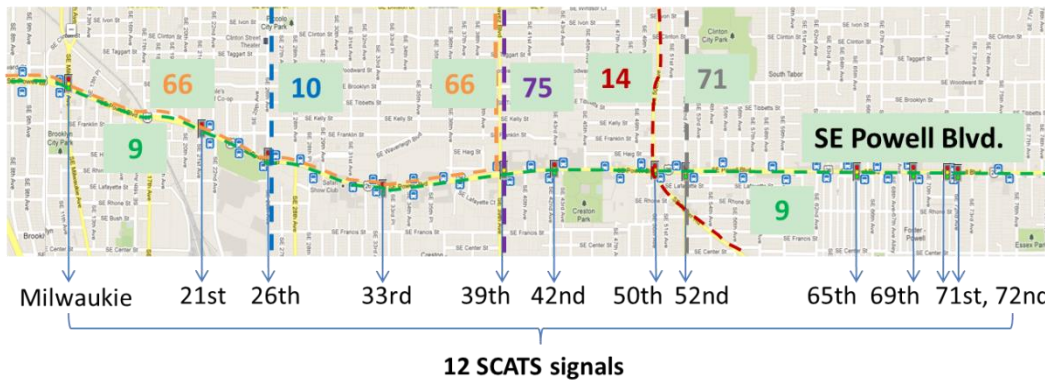


Figure 4. Transit lines along the study corridor.

To analyze the transit signal priority system performance, the bus stop event data, SCATS signal phase log data and traffic count data are integrated into one bus stop-to-stop trip database. A bus stop-to-stop trip is a bus trip between two consecutive bus stops that includes one SCATS signal. After data integration, each bus stop-to-stop trip includes attributes include bus stop activities (e.g. arrival time, departure time, schedule delay, passenger boarding/alighting, on-board passengers) at both bus stops, travel time and distance between bus stops and intersections, estimated bus arrival time at signalized intersections, estimated signal delay due to a red signal indication and/or time savings due to a transit signal priority (TSP) phase.

2.4 Roadside air quality data

In order to investigate the effects of detailed vehicle activity on near-road pollutant concentrations, high-resolution traffic data from the mid-block DWR detectors were used in concert with similarly high-resolution air quality measurements. Roadside air quality data were collected using portable instruments deployed during peak periods to measure sidewalk-level air pollution exposure concentrations. All instruments were placed on a portable table 2.5m from the roadway (see Figure 5). Data collection took place only in the absence of precipitation.



Figure 5. Portable roadside air quality monitoring setup

Data were collected at one second resolution and later aggregated to 10 seconds to match the output of the DWR traffic sensors. PM mass concentrations were measured with the TSI DustTrak (TSI Model 8533). The DustTrak measures three PM size designations: PM₁, PM_{2.5}, and PM₁₀, corresponding to PM with aerodynamic diameters below 1, 2.5, and 10 micrometers, respectively. Wind speed and direction were measured using an RM Young Ultrasonic Anemometer (Model 81000), and temperature and relative humidity are measured with a HOBO U12-013 (Onset).

2.5 On-road exposure concentration data

Assessment of air pollution intake requires combined knowledge of environmental, physiological, and travel conditions. Currently there is a lack of tools that allow integrated measurements of these data. In response, a portable, low-cost, multi-sensor device was recently developed and field-tested on the study corridor (as well as on other roadways in the area). The prototype device combines trajectory (location, speed, acceleration), local traffic (passing vehicles), air quality (CO, VOC), meteorology (temperature, humidity), and physiology (heart rate) data for travelers. The device connects wirelessly with a smartphone running a custom application that displays and logs the data, in addition to incorporating information from the smartphone's GPS receiver and third-party bio-monitors. Post-processing the space/time stamps

of these mobile data with the stationary traffic sensors on the corridor allows analysis relating the on-road measurements to traffic conditions. The prototype device is described in the documentation which is available for download along with the microcontroller and application source codes² (Bigazzi, 2013).

3 PERFORMANCE MEASUREMENT

3.1 Transit signal priority (TSP)

Transit signal priority (TSP) is the process of detecting transit vehicles approaching signalized intersections and adjusting the phasing of the signal in real time to reduce the delay experienced by the transit vehicle (Furth & Muller, 2000). The two most common TSP phases are green extension and early green (or *red truncation*).

Previous studies analyzed the impact of TSP systems on bus travel time savings, on-time performance, headways, and the delay and time savings for other vehicles. Due to the lack of disaggregated TSP phase log data and integrated analysis between signal phase log data with bus automatic vehicle location (AVL) and automated passenger count (APC) data, no study has evaluated TSP performance at the TSP phase level, assessing the effectiveness and efficiency of TSP phases for buses that request priority. TSP effectiveness of an intersection measures the percentages of TSP phases that are early, on-time or late to a bus when it arrives at an intersection. For example, it is possible that 20 buses requested priority at an intersection, ten TSP phases were triggered, five, three, and two of them were granted early, late and on-time (beneficial) to the buses, respectively. TSP efficiency of a TSP phase assesses the passenger time savings and vehicle delay per second of TSP phase duration. These disaggregated TSP performance analysis can help the cities and transit agencies to better understand the existing TSP system performance, identify potential problems and improvement opportunities.

Figure 6 shows the average number of bus trips per day that did and did not request TSP from both directions at intersections between 26th Ave. and 72nd Ave. along Powell Blvd. It shows that almost half of the bus trips requested TSP at each intersection. Because there are no bus emitter activation/deactivation records, a bus is determined to have requested priority if the bus actual departure time is more than 30 seconds late than the scheduled departure time.

² <http://alexbigazzi.com/PortlandAce/>

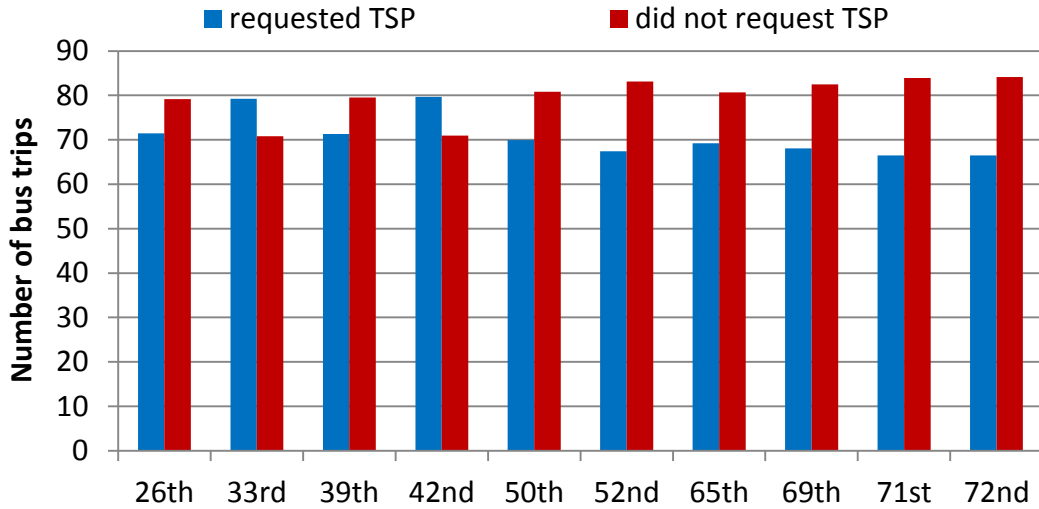


Figure 6. Average number of bus trips per day.

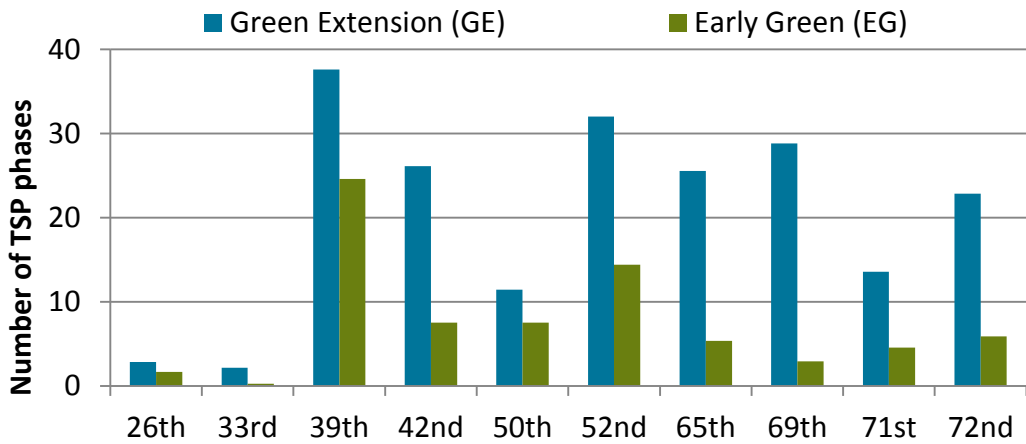


Figure 7. Average number of TSP phases per day.

Figure 7 shows the average numbers of green extension phases and early green phases per day. It shows that few TSP phases were granted at the intersections of 26th Ave. and 33rd Ave. on Powell Blvd., which indicates a potential TSP setting problem at these two intersections. There are more green extension phases than early green phase. The average durations of green extension and early phases are 7 and 11 seconds, respectively. Figure 6 and Figure 7 show that the average number of TSP requests is much higher than the number of TSP phases at each intersection. Therefore, not all of the TSP requests triggered the granting of a TSP phase.

3.1.1 Data Integration

Integrating the bus AVL/APC data with the SCATS signal log data and vehicle count data is important because it provides the required information for TSP performance analysis. It is

also a challenging step because the bus AVL/APC data and SCATS data are collected in different spatial dimensions. Bus AVL/APC data are collected at bus stops while SCATS data are collected at intersections. Bus trajectory information is unknown between bus stops. However, TSP performance analysis at the TSP phase level requires bus arrival time information at the intersections. Therefore, this study developed an algorithm to estimate the probabilistic bus arrival times at an intersection based on: 1) empirical bus travel speed probability distribution; 2) bus departure and arrival time at the upstream and downstream stops of an intersection; and 3) the signal phase start and end times of that intersection. These estimated bus arrival time probability distributions are used to estimate TSP performance measures. Based on this algorithm, we integrated the three data sources into one “bus stop-to-stop trip” database. Each bus stop-to-stop trip is a data record, and each bus stop-to-stop trip is associated with some input information and output attributes. Table 1 lists the input data and output attributes for each bus stop-to-stop trip record. The input data are from the three original data sources, the output variables are estimated based on the algorithm.

Table 1. Bus stop-to-stop trip attributes

Input Data	Output Variables
Upstream/downstream distance	Priority request
Bus departure/arrival time at the upstream and downstream stops	Probabilities of bus arriving time at intersection during green/red/green extension/early green
Passenger boarding/alighting/load	Bus signal delay
Signal phase start/end times	Bus time saving due to a TSP phase
Traffic volumes	Non-bus vehicles time saving/delay due to a TSP phase

In the output variables in Table 1, “priority request” indicates whether a bus requested priority. Given the bus departure and arrival time at the upstream and downstream stops and the signal phase start/end time of an intersection, probabilities of the bus arriving at the intersection during green, red, green extension and early green phases can be estimated. This information can be used to estimate the effectiveness of TSP phases. Based on this information, signal delay for a bus stop-to-stop trip can also be estimated. The expected time saving for a bus due to TSP phase can be estimated, and the expected time saving for other vehicles on the main street and expected delay for other vehicles on the side street can also be estimated.

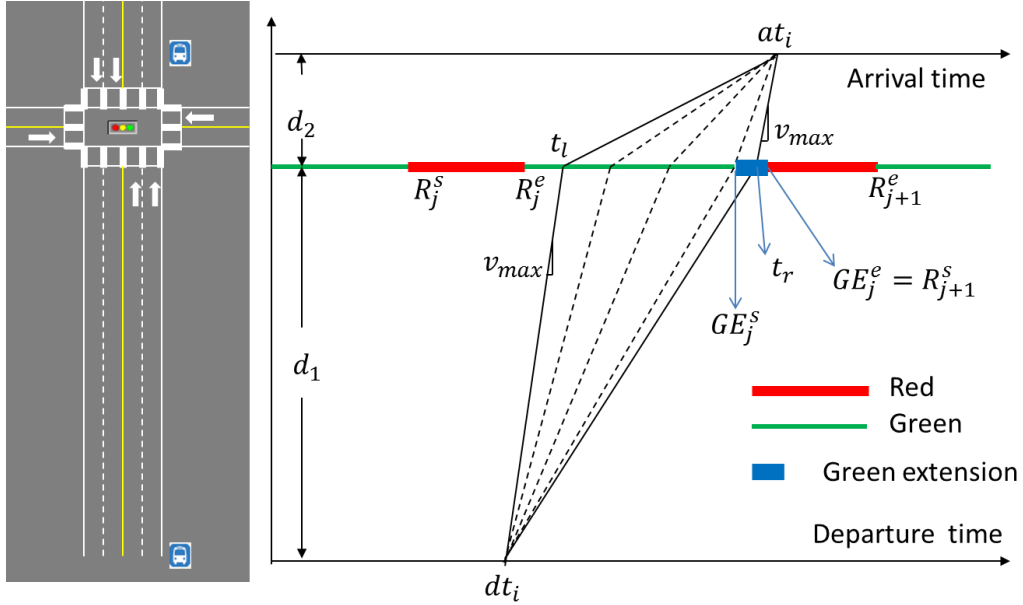


Figure 8. Feasible bus stop-to-stop trip trajectories with an early green phase

Figure 8 shows an example of a bus stop-to-stop trip in a time-space diagram. d_1 and d_2 represent the distance between the upstream bus stop and the intersection stop bar, and the distance between the intersection stop bar and the downstream bus stop; dt_i and at_i are the departure time from the upstream stop and the arrival time at the downstream stop for bus trip i ; R_j^s and R_j^e are red phase start time and end time in cycle j ; GE_j^s and GE_j^e are early green phase start time and end time in cycle j . Although the true bus trajectory is unknown, based on the bus travel speed probabilistic distribution for each stop-to-stop segment, a feasible bus trajectory boundary can be drawn in the time-space diagram given dt_i and at_i . t_l and t_r are the earliest and latest possible times that bus trip i could have arrived at the intersection given dt_i and at_i . Based on the probability distribution of bus travel speeds, the expected signal delay of bus i and the expected time saving due to the green extension phase can be estimated. The equations for estimating these output variables are omitted for simplicity.

3.1.2 TSP Effectiveness

In this study, if a TSP phase is granted in the same cycle when a bus arrives at the intersection and this bus requested priority, this TSP phase is granted in time to the bus that requested priority, and this TSP request triggers a TSP phase granted in time. The timely cycles are defined differently between green extension (GE) and early green (EG) phases so that the

TSP phase is close to the middle of a timely cycle. As shown in Figure 9, a timely cycle for a GE phase is the time interval between two consecutive green phase start times, and a timely cycle for an EG phase is the time interval between the middle time of two green phases. In Figure 9 (a) and (b), a bus “d” arrives at the intersection in cycle ① but a TSP phase is granted in cycle ②; therefore, this TSP phase in cycle ② is not triggered by any bus. Bus “a”, “b” or “c” arrives at the intersection in cycle ③ and each could have triggered the TSP phase. This TSP phase in cycle ③ is granted late, on-time and early to bus “a”, “b” and “c”, respectively. However, only when a TSP phase is granted on-time to a bus that requested priority, it is considered effective. Therefore, whenever there is a TSP phase granted, it is possible that: 1) no bus triggered this TSP phase within a cycle length; 2) this TSP phase is late to a priority request; 3) it is on-time to a priority request; and 4) it is early to a priority request.

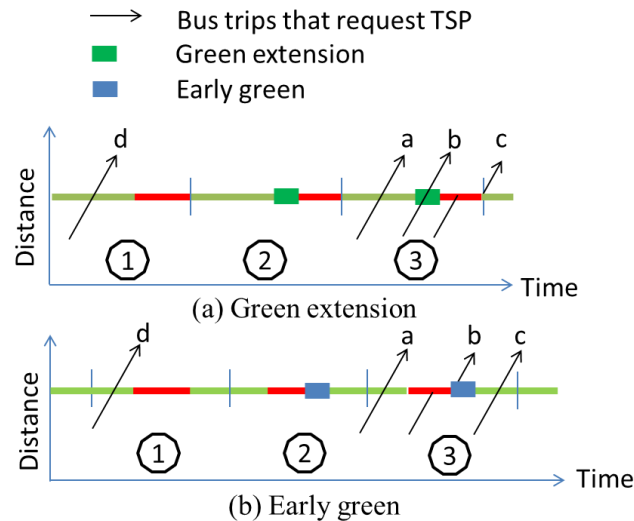


Figure 9. TSP timeliness and effectiveness illustration.

Based on the estimated probabilities that buses arrive at an intersection during the green, red, green extension and early green phases, the percentages that a TSP phase was granted early, on-time, late and in a different cycle to a TSP request are shown in Figure 10 (a) and (b).

Results vary significantly across intersections and by direction. Figure 10 (a) shows that, on average, 64% of the GE phases are late, 28% of them are granted in a different cycle and 5% of them are on-time. This means that 95% of GE phases are not effective and most of them are late. Results clearly indicate a problem with the GE phases. This might be a TSP control strategy problem or a TSP request detection/deactivation problem. Figure 10 (b) shows that, on average,

an EG phase has 40% probability of being on-time, 30% probability of being early and 28% probability of being in a different cycle. Therefore, EG phases are much more effective than GE phases.

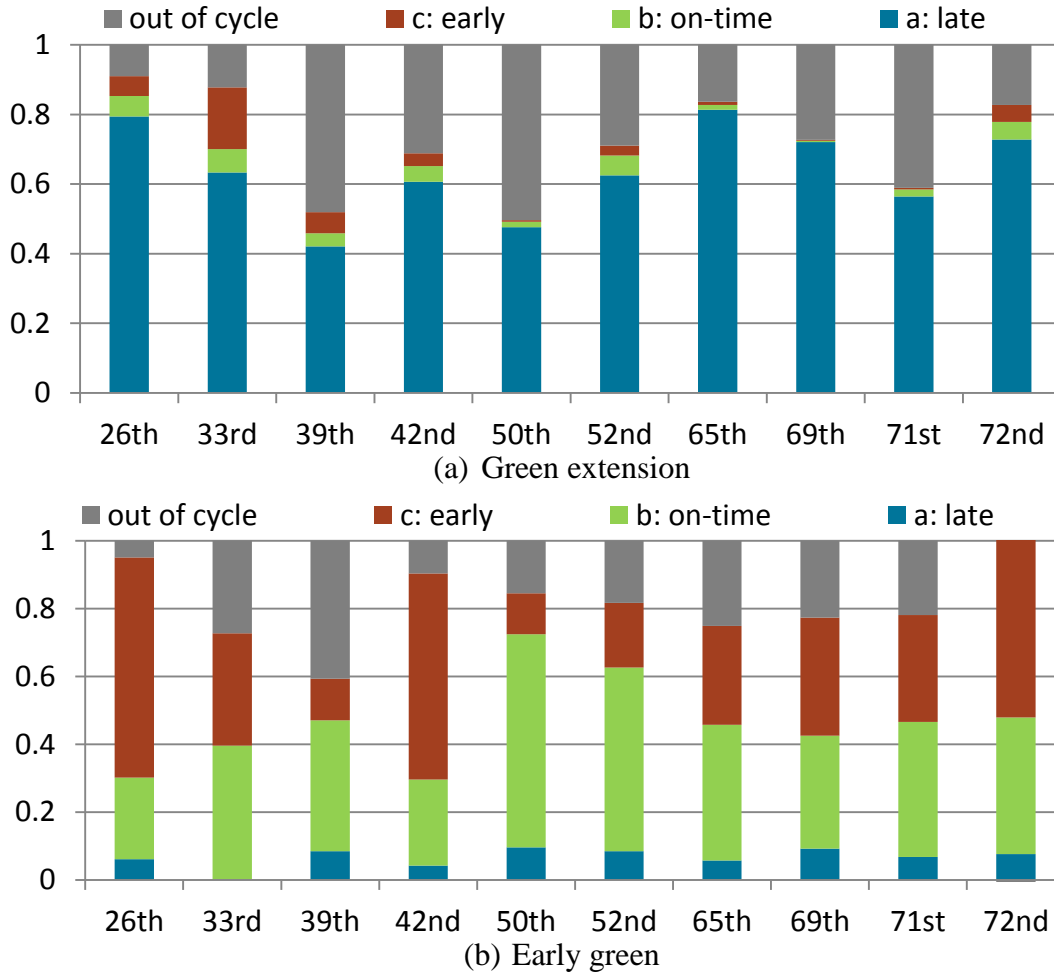


Figure 10. TSP phase effectiveness.

3.1.3 TSP Efficiency

A bus can benefit from a GE phase only if the bus arrives at an intersection during the GE phase; on the other hand, a bus can benefit from an EG phase if the bus arrives at the intersection during regular red time or the EG phase. However, if a bus benefits from a GE phase, the time savings will be the time interval between the arrival time of this bus at the intersection and the end time of the following red phase. If a bus benefits from an EG phase, the maximum time savings will be the EG phase duration. Because red phase duration is longer than EG phase

duration in most of the intersections, the time savings for a bus that benefits from a GE phase is usually higher than when it benefits from an EG phase. Therefore, it is important to measure the time savings for buses and onboard passengers per TSP phase. It is also necessary to assess the time savings for non-bus vehicles on the major street and vehicle delays on the minor street due to a TSP phase. Also, because the average GE and EG phase durations are different across intersections, the time savings and delay per second TSP phase will be compared.

For each bus stop-to-stop segment, the average bus passenger time savings per second TSP phase can be estimated by:

$$\frac{\sum_{i \in I} PTS_{GE_i}}{\sum_{j \in J} GE_j^e - GE_j^s}, \frac{\sum_{i \in I} PTS_{EG_i}}{\sum_{j \in J} EG_j^e - EG_j^s} \quad [1]$$

Figure 11 (a) and (b) show that the estimated total passenger time savings per second GE phase is much lower than EG phase. Therefore, early green phases are more efficient than green extension phases in most of the intersections. This may be because there are too many GE phases that are not beneficial to any buses.

According to (Smith, Hemily, & Ivanovic, 2005), TSP works better at far-side stops because bus arrival time prediction is more reliable at far-side stops. However, Figure 11 (a) and (b) do not show clear differences between near-side and far-side stops. This finding does not indicate that near-side and far-side stop configurations have no impact on TSP performance, because there are only six near-side stop segments, and five of them may have TSP settings problems.

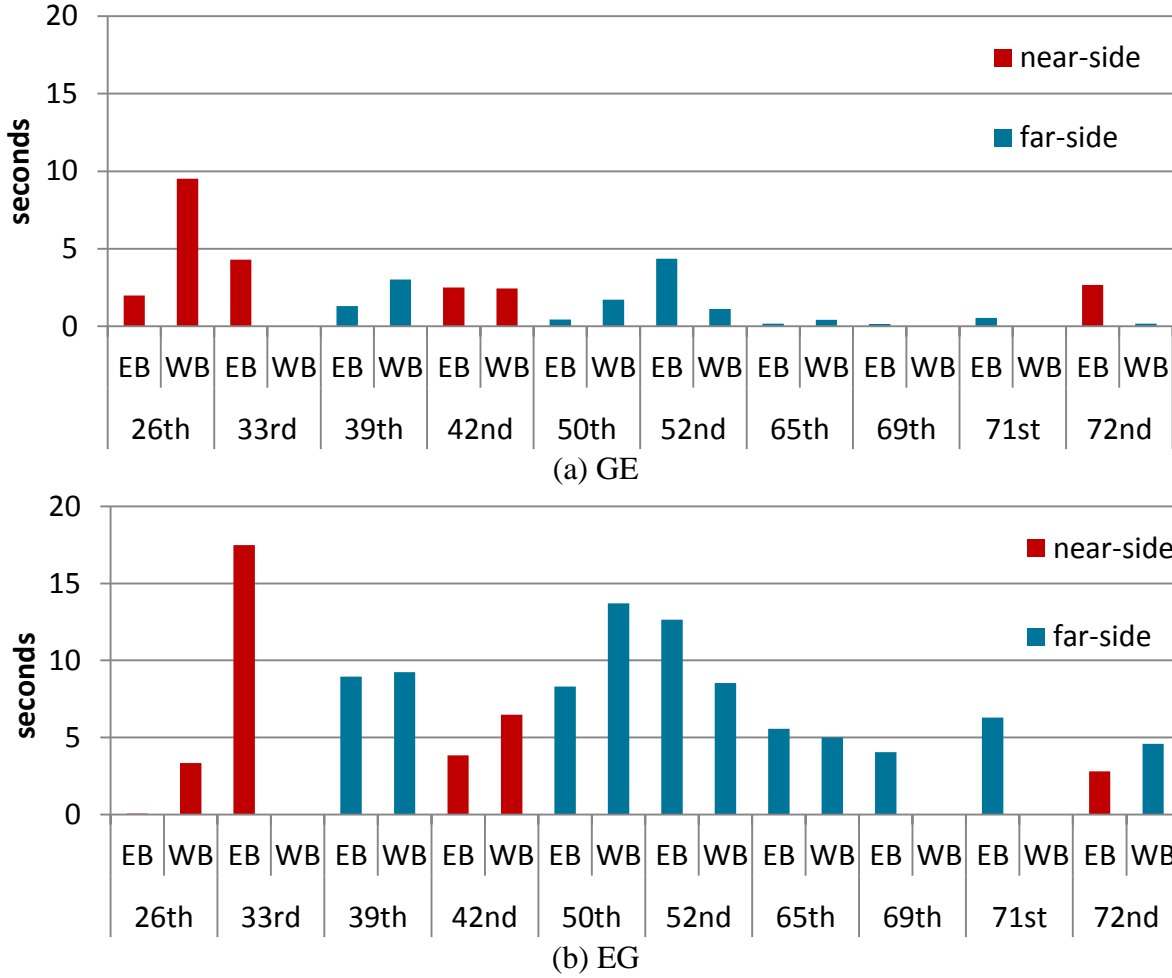


Figure 11. Estimated total passenger time savings per second TSP phase.

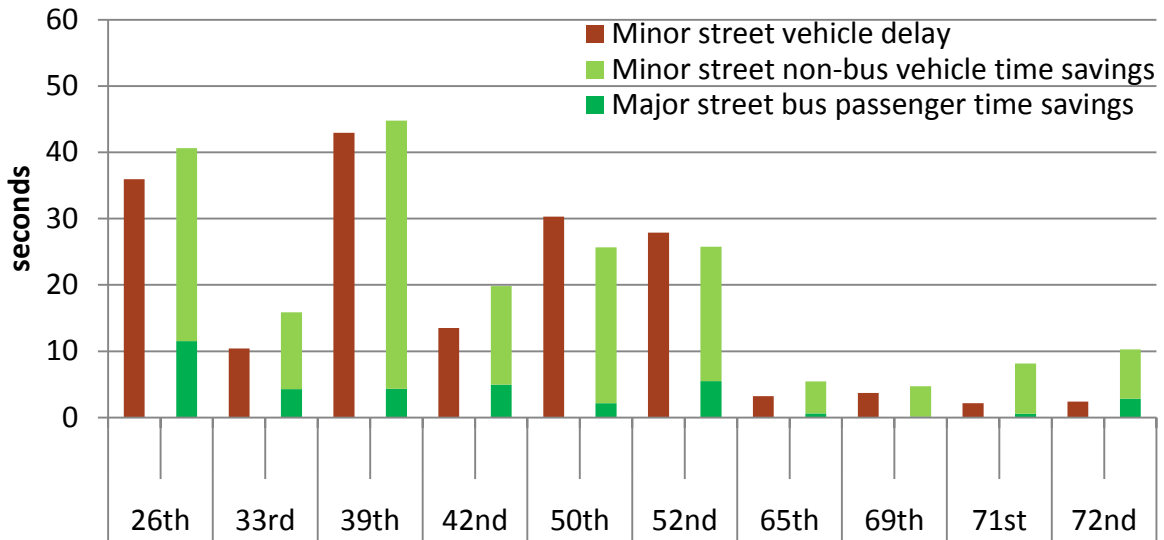
Assuming vehicles arrival rate at intersections are uniform (vehicle platooning arrival pattern was not considered in this case), traffic conditions are unsaturated in all four approaches, and regular green phase and red phase durations will not change if a GE phase or an EG phase is granted, the total time savings (TTS) for non-bus vehicles on the major street and the total delay (TD) for vehicles on the side street can be estimated by the following equations:

$$TTS = \frac{q_1 \cdot q_2}{2(q_2 - q_1)} (2 \cdot Red \cdot TSP - TSP^2) \quad [2]$$

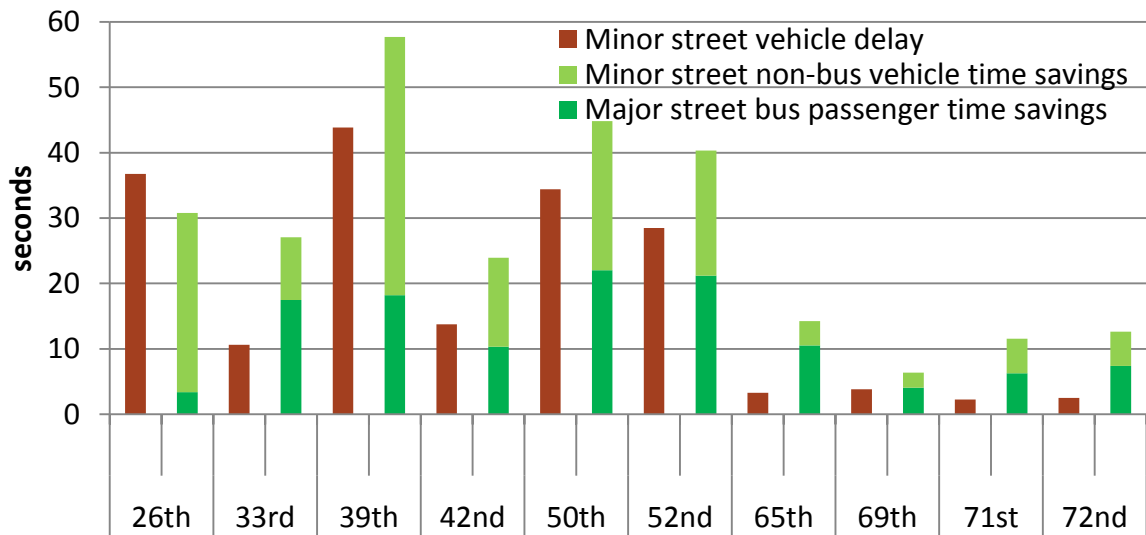
$$TD = \frac{q_1 \cdot q_2}{2(q_2 - q_1)} (2 \cdot Red \cdot TSP + TSP^2) \quad [3]$$

Assuming all non-bus vehicles are single occupancy vehicles, results are shown in Figure 12. Results show that the total time savings and delays for non-bus vehicles per second GE phase

and per second EG phase are very similar (less than 2 seconds difference), which means the nonlinear effect of TSP phase duration on non-bus vehicles time savings and delays is negligible. For each second EG phase, the bus passenger time savings is slightly less than the total vehicle delay on the side street for intersections west of 52nd Ave., but the sum of the bus passenger time savings and the total vehicle time savings on the major street is much higher than the side street vehicle delay at all intersections. For each second GE phase, the sum of bus passenger time savings and non-bus vehicle time savings on the major street is almost equal to the vehicle delay on the side street.



(a) Green extension



(b) Early green

Figure 12. Total passenger time savings and vehicle delays per second TSP phase.

3.2 Signal operations and roadside air quality

The relationship between traffic operations and air quality was studied using aforementioned air quality, meteorological, and traffic measurement devices. Specifically, fine particulate matter (PM_{2.5}) was measured at a mid-block location between two traffic signals during a morning peak period, directly in line with a DWR sensor measuring vehicle volume, speed, and lane occupancy.

Data were analyzed at 10-second intervals, a much finer resolution than comparable roadside air quality study designs. This resolution allowed special attention to be paid to changes

in traffic conditions, including fleet mix, queuing, and vehicle platooning. Significant correlations were observed between vehicle platoons and increases in $PM_{2.5}$ concentrations.

During the data collection period, substantial congestion in the morning commute direction (westbound) resulted in a breakdown in traffic flow. Average westbound speeds were about 30mph at the start of the study period (7:00am), but quickly dropped to below 10mph and did not improve by the end of the study period (9:00am). The availability of high resolution traffic data from the DWR sensor allowed the investigation of traffic state-pollutant concentration analysis. Two types of traffic states were explored: the onset of congestion and the periodic arrival of vehicle platoons from upstream signals.

3.2.1 Congestion Identification

Traffic volume data indicate the number of vehicles present near the air quality monitoring site, but they do not necessarily indicate the traffic state. That is, whether a roadway is congested or not. A method derived from Bertini (2003) was employed to empirically identify traffic states in which two states are identified: congested and uncongested. Cumulative speeds, $N(t)$, were plotted against time (top row in Figure 13). The curve's slope at time t represents the vehicle speed at that time. A rescaled cumulative (oblique) speed curve (bottom row in Figure 13) amplifies changes in speed to emphasize the moment of speed reduction. The oblique speed curve was created by reducing $N(t)$ from $v_0 t$, where v_0 is an oblique scaling rate.

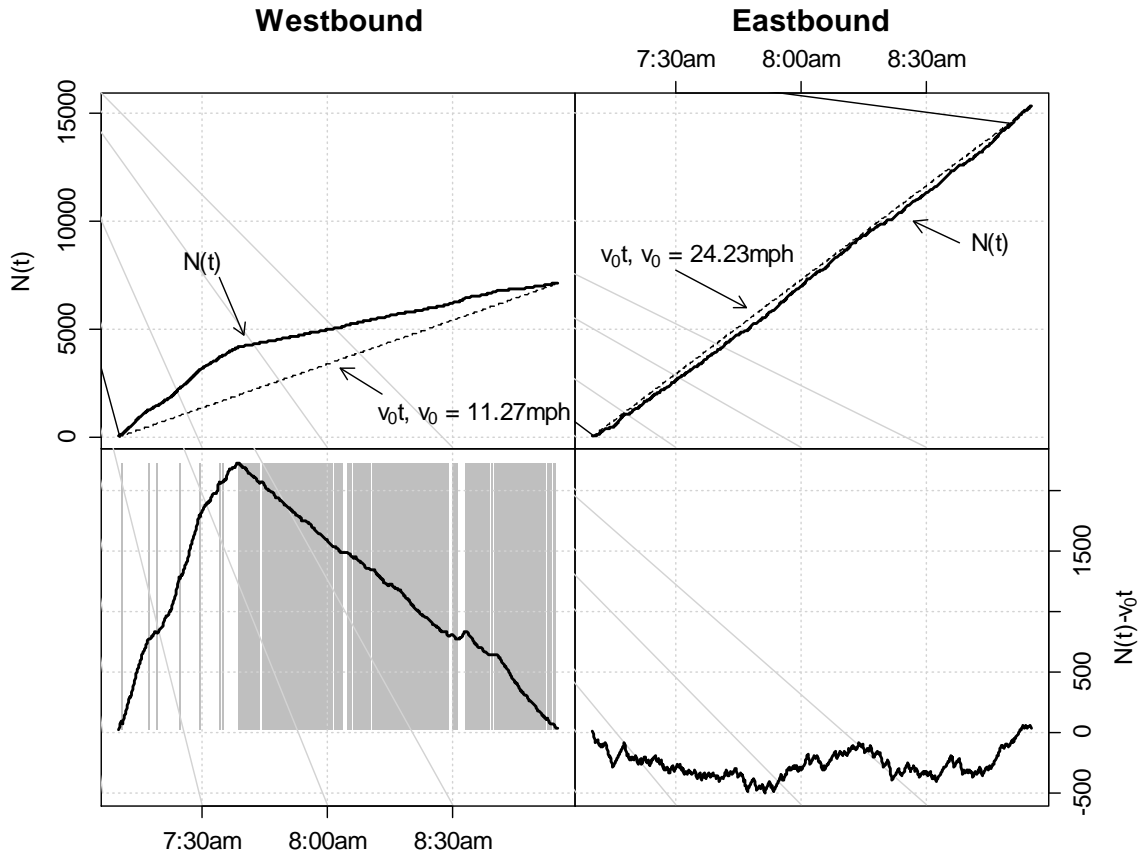


Figure 13 Rescaled cumulative (oblique) speed curve construction using cumulative speeds, $N(t)$, and oblique cumulative speeds, $N(t) - v_0t$. Shaded area indicates active queue.

A local maximum on the oblique speed curve indicates a time at which a speed reduction occurred, and a local minimum indicates a time at which a speed increase occurred. The two conditions are, in this context, referred to as queuing activation and deactivation points, respectively. The shaded portion of the oblique speed curve indicates an active queue. The onset of congestion was identified at 7:38am. From that point, the queue was primarily active, indicating congestion. No congestion occurred in the eastbound direction.

Median $PM_{2.5}$ concentrations were compared before and after the onset of congestion (see Figure 14). Boxplots of the concentrations indicated lower median concentrations for active queuing periods prior to congestion than for inactive periods. In contrast, higher median concentrations were observed for active queuing periods after the onset of congestion than for inactive periods.

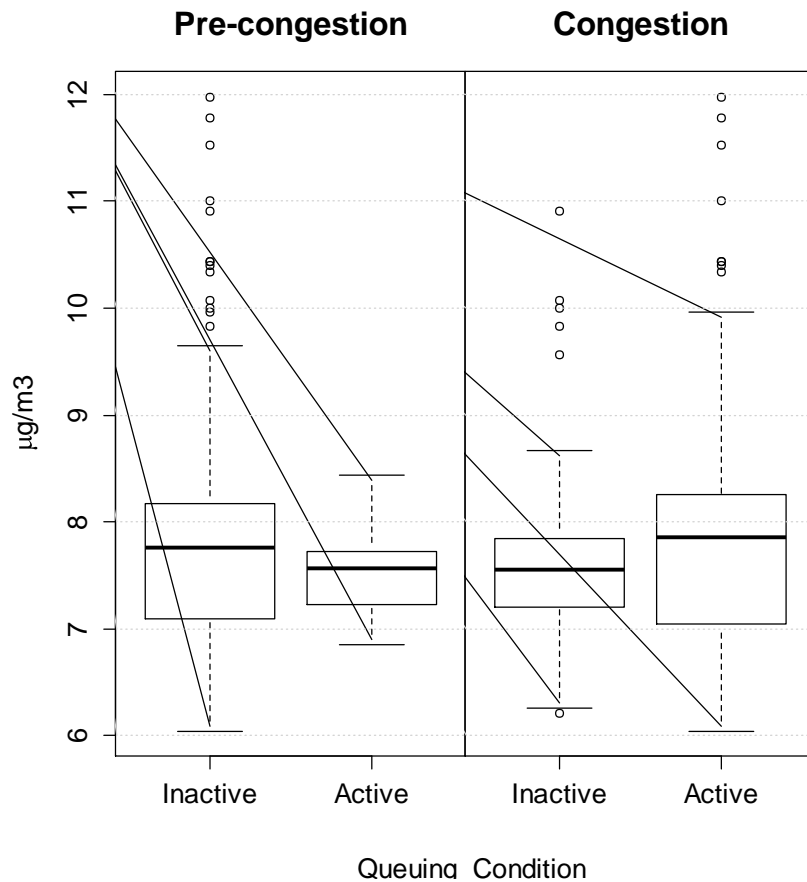


Figure 14 PM_{2.5} concentrations at different congestion and queuing conditions

Active queuing periods after the onset of congestion may differ from those prior to congestion, helping to explain the discrepancy in median PM_{2.5} concentrations. Prior to the onset of congestion, active queuing periods are characterized by brief decreases in speed, though for time durations too short to bring traffic to congested conditions. Short queuing periods outside of congestion, then, likely lead to traffic conditions with lower accelerations, which may result in lower emissions rates and lower PM_{2.5} concentrations.

3.2.2 Vehicle Platoon Identification

The cyclic nature of vehicle presence in the study due to the upstream traffic signals was detectable in the traffic volume data using autocorrelation function (ACF) and partial autocorrelation function (PACF) plots. ACF and PACF plots illustrate the similarities between observations as a function of the time lags between the observations (see Figure 15). Both of these functions are commonly used as a method for determining repeating patterns.

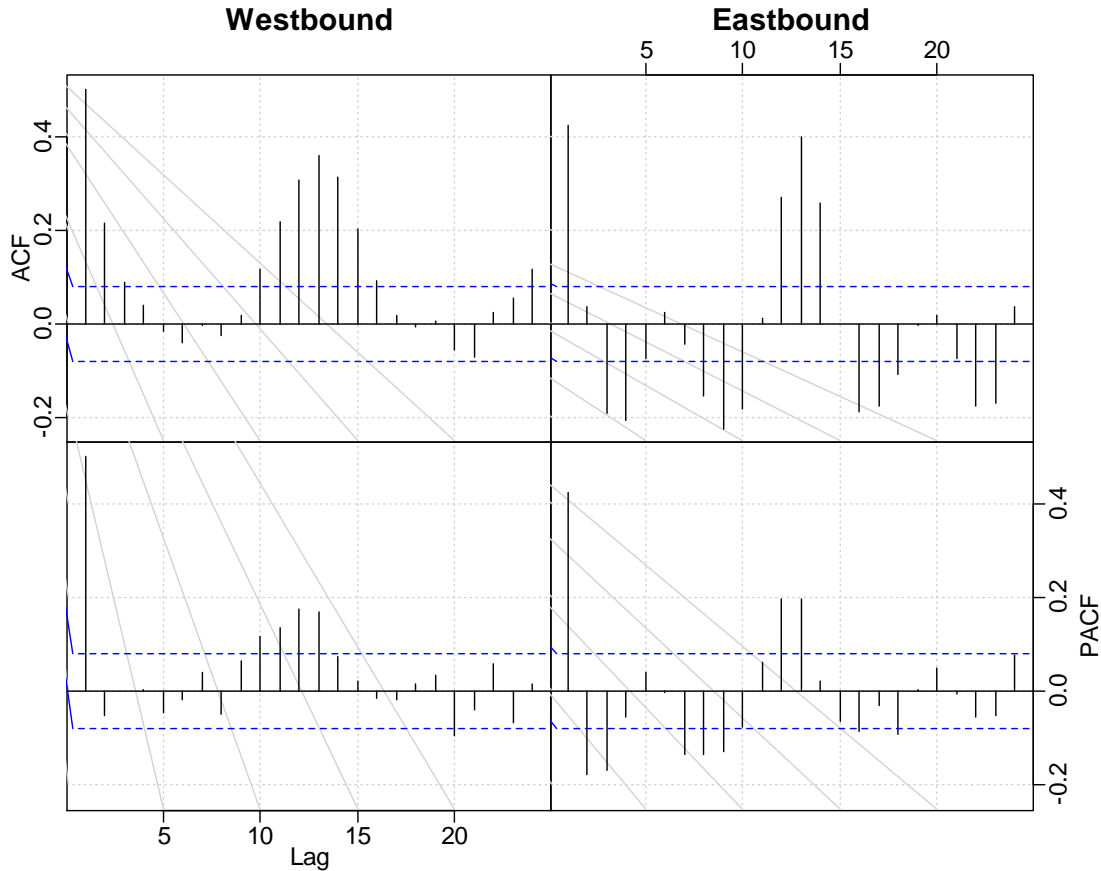


Figure 15 Autocorrelation of vehicle volumes showing vehicle platooning with upstream signal cycles (1 lag = 10 seconds)

The westbound upstream signal had a median cycle length of 123 seconds, and the eastbound signal had a median cycle length of 125 seconds. Thus, vehicle platoons would be expected to arrive every 123 and 125 seconds from their respective directions. These cycles are evident in the vehicle volume ACFs and PACFs in Figure 15. One lag in the figure equals 10 seconds, and the eastbound response has a clear spike at 13 lags, or 130 seconds, due to traffic platooning. The westbound direction had a slightly more dampened response, likely due to the substantial congestion, which mitigated any upstream cycle effect due to the constant vehicle presence at the sensor location.

To investigate the effect of vehicle platooning on roadside $PM_{2.5}$ concentrations, a cross-correlation function (CCF) was made for both directions of travel. The CCF in Figure 16 illustrates correlations between $PM_{2.5}$ concentrations at time t and traffic volumes at time $t + h$, for $h=0, \pm 1, \pm 2, \pm 3, \dots$. Negative values for h indicate a correlation between volumes at a time h

units before t and $PM_{2.5}$ concentrations at time t . The dashed lines indicate the statistical significance level. No westbound correlations were significant; westbound vehicle platooning did not have a significant effect on $PM_{2.5}$ concentrations. In the eastbound direction of travel, $PM_{2.5}$ concentrations were significantly positively correlated (+10.4%) with vehicles passing at 12 lags, or 120 seconds. This lag time roughly matched the upstream cycle length, and the eastbound vehicle ACF and PACF. Eastbound vehicle platooning, then, significantly positively correlated with $PM_{2.5}$ concentrations. It is likely that platooning conditions were easier to identify in the eastbound direction due to the uncongested conditions and clear vehicle arrival times for the duration of the study period.

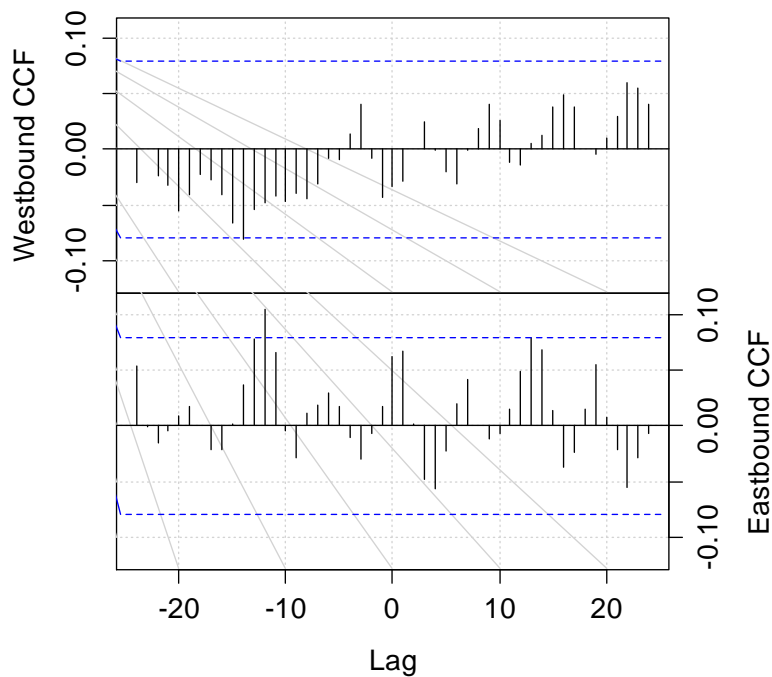


Figure 16 Cross-correlation of vehicle volumes with $PM_{2.5}$ concentrations (1 lag = 10 seconds)

3.3 On-road exposure risk and traffic conditions

Travelers' health risk from air pollution is one dimension of a roadway's environmental performance. Although most research focuses on exposure concentrations, ventilation is also an important determinant of pollutant inhalation and uptake – particularly for active travelers such as pedestrians and bicyclists (Bigazzi & Figliozzi, 2014). In order to connect a roadway's

functional and operational condition with pollutant inhalation risks, three dimensions of data are needed:

1. Travel and traffic conditions (location, facilities)
2. Environmental conditions (pollutant concentrations, weather)
3. Physiological conditions (traveler's ventilation rate)

Figure 17 is an example of the information that can be gained from integrating high-resolution environmental and physiological measurements. Figure 17 shows second-by-second data from a 7.9 km (4.9 mi) bicycle trip along the study corridor starting from an inner commercial/industrial area (from right to left) on July 11, 2013, with the measured exposure shown as the pin height and the bicyclist's breathing rate shown as the pin color (with lower to higher rates shown as red-yellow-orange-green). Exposure "hot-spot" areas with jointly higher ventilation and concentration values can be identified by tall green pins. The sample trip in Figure 17 started with high concentrations but relatively low ventilation in the commercial/industrial area. The largest exposure "hot-spot" occurred after crossing SE 39th Ave (marked on the figure with a red box). This location has high traffic volumes and an upward grade, where we would expect both greater vehicle emissions and greater bicyclist exertion.



Figure 17. Integrated travel (location), environmental (pollutant concentration as pin height), and physiology (breathing rate as pin color, where green is high) data; exposure hot-spots can be identified by tall green pins (such as outlined in red)

(map imagery from Google Earth)

In order to examine the effect of traffic on exposure risks, the on-road data were mapped to the roadway network and synchronized with the traffic data. GPS data points were mapped by proximity to a link-based GIS layer from the City of Portland that included estimated ADT for

each link based on interpolated traffic count data. Figure 18 shows correlation coefficients between ADT and 10-second aggregated exposure and physiology data from 12.5 hours on a variety of mixed-traffic roadways in the area (not only the Powell Blvd. study corridor, which has roughly consistent ADT along its length). All data were collected between April and September, 2013 near the morning peak period (7-10 am). On-road exposure is shown for carbon monoxide (CO) and volatile organic compounds (VOC) sensors; on-road physiology is shown for heart rate and breathing rate. Correlation coefficients are indicated by the color shading of the cell, and significant coefficients based on two-tailed t -tests ($p < 0.05$) are also printed in text.

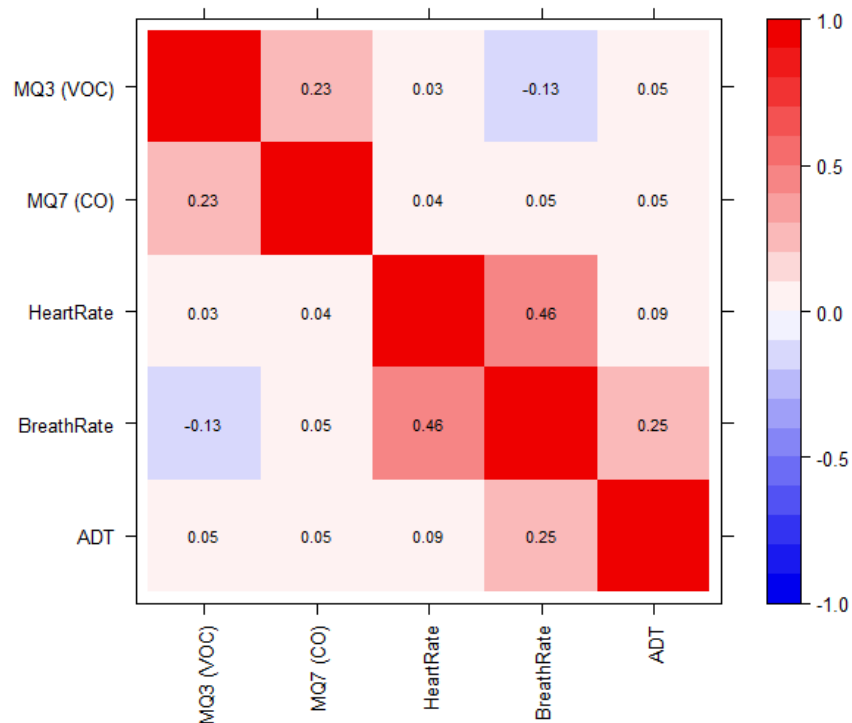


Figure 18. Correlation coefficients for 10-second aggregated data from all mixed-traffic roadways (significant relationships at $p < 0.05$ are marked with text; $N = 4,500$)

The two exposure variables are significantly positively correlated with each other, as are the two physiological variables, as expected. Exposure and physiology are both positively correlated with ADT, though the correlation with physiology is stronger. Bicyclist self-determined speed was found to be higher on larger roads, which is consistent with the physiology/ADT relationship.

Concurrent traffic conditions for the on-road data were determined by matching time-stamps with the DWR data set described above. Figure 19 shows correlation coefficients among three DWR traffic variables (volume, speed, and density) and the four on-road data variables from the previous figure. A subset of only on-road data from the study corridor is included (1.5 hours). Correlation coefficients are indicated by the color shading of the cell, and significant coefficients ($p < 0.05$) are also printed in text.

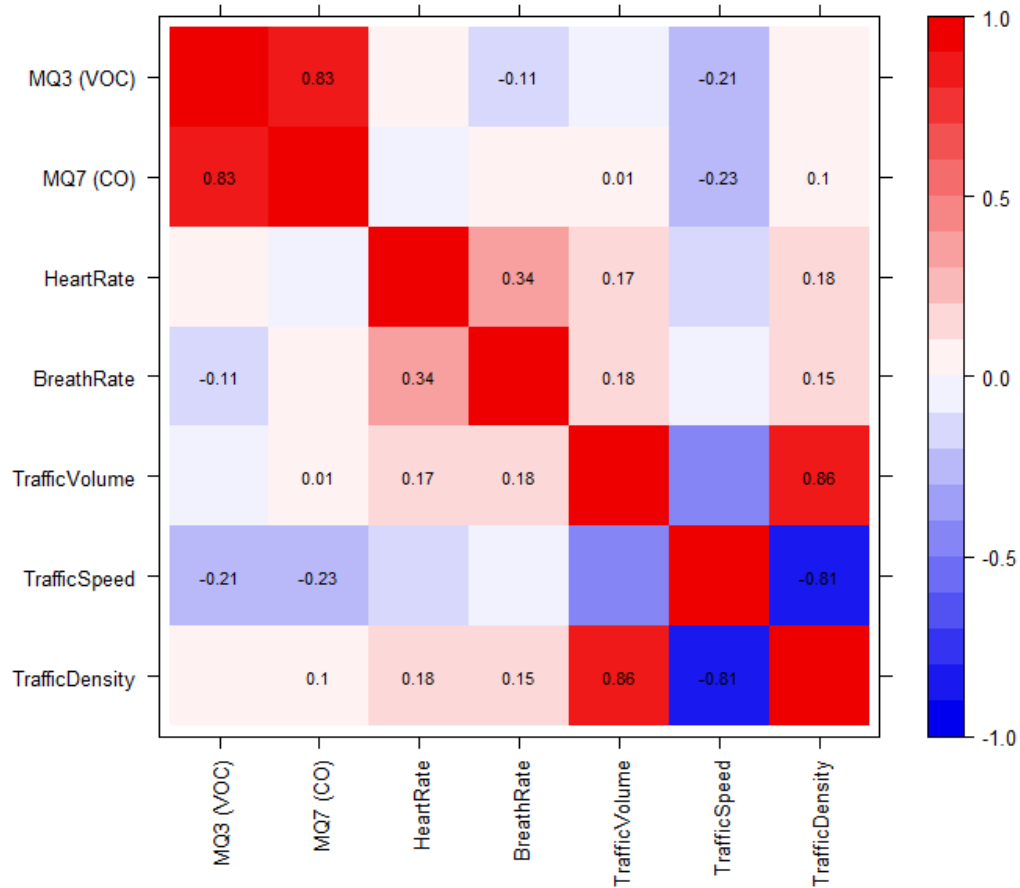


Figure 19. Correlation coefficients for 10-second aggregated data while riding on Powell Blvd. (significant relationships at $p < 0.05$ are marked with text; $N = 528$)

Amongst the traffic variables, density was significantly correlated with volume and (negatively) with speed. The insignificance of the volume-speed correlation could be due to the non-linear shape predicted from traffic flow theory (May, 1989). Traffic speed was negatively correlated with exposure concentrations; concentrations were higher during congestion when speeds were low. Traffic volume and density were only significantly correlated with CO, not

VOC. Traffic volume and density were positively correlated with physiology, though the traffic speed/physiology correlation was not significant. Overall, both high-volume facilities and congested periods (with low traffic speeds and high traffic density) were associated with higher pollution risks due to exposure concentration and ventilation.

4 CONCLUSIONS

This paper presents three analyses with unique findings that arise from combining fixed and mobile transportation data sources. Assessment of the performance of a transit signal priority system required a combination of traffic signal timing data and on-bus location data to determine the signal status when buses arrived at intersections. Vehicle volume data were also used to quantify the time trade-offs for bus and auto passengers on the major arterial road and cross roads. A study of roadside air quality combined fixed-site traffic data with data from a deployable air monitoring station to quantify the high-resolution impact of traffic characteristics on near-road air quality. The third analysis combined on-road mobile air quality and physiology data with stationary traffic data to reveal correlations between on-road exposure risk and traffic characteristics across both space (ADT on different links) and time (varying traffic levels on one facility).

Fixed and mobile data integration requires synchronization and aggregation in both space and time dimensions. The data processing for these analyses was *ad hoc* and manual. In order to realize the potential of emerging transportation data sources, the combination of high-resolution fixed and mobile data types must become a less resource-intensive activity. One possibility for facilitating these data integrations is increased flexibility and use of archived data user services (ADUS) such as PORTAL in Portland, Oregon (Tufté et al., 2010). ADUS architectures could aid analysts by providing enhanced synchronization, aggregation, and integration functions for a wider range of data sources.

5 REFERENCES

Bertini, R. L. (2003). Toward the systematic diagnosis of freeway bottleneck activation. In *2003 IEEE Intelligent Transportation Systems, 2003. Proceedings* (Vol. 1, pp. 442–447 vol.1). doi:10.1109/ITSC.2003.1251993

- Bigazzi, A. Y. (2013, July). The Portland ACE Documentation: a Portable, Low-cost, and Networked Device for Assessing Cyclists' Exposure. Portland State University. Retrieved from <http://alexbigazzi.com/PortlandAce/>
- Bigazzi, A. Y., & Figliozzi, M. A. (2014). Review of Urban Bicyclists' Intake and Uptake of Traffic-Related Air Pollution. *Transport Reviews*, 34(2), 221–245. doi:10.1080/01441647.2014.897772
- Feng, W., Bigazzi, A., Kothuri, S., & Bertini, R. (2010). Freeway Sensor Spacing and Probe Vehicle Penetration. *Transportation Research Record: Journal of the Transportation Research Board*, 2178(-1), 67–78. doi:10.3141/2178-08
- Furth, P., & Muller, T. H. (2000). Conditional Bus Priority at Signalized Intersections: Better Service with Less Traffic Disruption. *Transportation Research Record*, 1731, 23–30.
- May, A. (1989). *Traffic Flow Fundamentals*. Prentice Hall.
- Smith, H. R., Hemily, P. B., & Ivanovic, M. (2005). *Transit Signal Priority (TSP): A Planning and Implementation Handbook*. ITS America. Retrieved from <http://www.fta.dot.gov/documents/TSPHandbook10-20-05.pdf>
- Tufte, K., Bertini, R., Chee, J., Fernandez-Moctezuma, R., & Periasamy, S. (2010). Portal 2.0: Towards a Next-Generation Archived Data User Service. In *Proceedings of the 89th Annual Meeting of the Transportation Research Board*.